Visual Fatigue Prediction for Stereoscopic Image

Donghyun Kim, *Student Member, IEEE,* and Kwanghoon Sohn, *Member, IEEE*

***Abstract*—In this letter, we propose a visual fatigue prediction metric which can replace subjective evaluation for stereoscopic images. It detects stereoscopic impairments caused by inappropriate shooting parameters or camera misalignment which induces excessive horizontal and vertical disparities. Pearson's correlation was measured between the proposed metrics and the subjective results by using *k*-fold cross-validation, acquiring ranges of 78–87% with sparse feature and 74–85% with dense feature.**

***Index Terms*—Disparity, stereoscopic image, visual fatigue.**

I. Introduction

A NUMBER of studies have shown that stereoscopic displays provide psychological impacts and improved representation capabilities that allow the user a better understanding of the visual information being presented [1]. However, the success of 3-DTV should be followed by the steady and constant effort for high quality and comfortable content with an enhanced understanding of human visual characteristics.

There are two primary problems causing unwanted effects in 3-DTV: depth distortion and visual fatigue. Depth distortion is a phenomenon in which watching the scene in stereoscopic display differs from viewing the scene directly. This is an unavoidable issue, except for the case of ortho-stereoscopy. The second problem of 3-DTV is visual fatigue. In [2] and [3], visual fatigue induced by the conflict between accommodation and convergence is reviewed. Moreover, visual fatigue is also caused by a number of other factors which include camera configuration, viewing conditions, and image characteristics, magnitude of parallax, parallax distribution, parallax variation, vertical parallax, crosstalk, noise, motion, and asymmetries.

There have been several studies investigating the effects of camera configuration. Ijsselsteijn *et al.* [4] investigated the effects of camera separation, convergence distance, and focal length. The issue of visual fatigue induced by excessive parallax over the fusional range has been studied in several publications [5]–[8]. Excessive parallax often occurs because of the content creator's desire to provide a more powerful 3-D impact. Moreover, excessive parallax occurs when the viewing circumstances or the target display are changed. Kooi and Toet [5] measured comfort from a wide range of distortions, including spatial distortion, asymmetries, and disparities. In addition, 3-D consortium established safety guidelines for creating comfortable 3-D contents [6]. The fusional range was studied as a function of viewing distance and display field of view in [7] and as a function of disparity and spatial frequency in [8].

In [9], visual fatigue was predicted using an analysis of parallax distribution by dividing the image into nine regions. Effects of parallax variation can be found in [10]–[12]. Ijsselsteijn *et al.* [10] indicated that presence ratings were subject to considerable temporal variation. Nojiri [11] and Okano [12] studied how visual comfort was affected by the range of parallax distribution and temporal parallax changes.

Many researchers have reported that vertical parallax causes visual fatigue and eyestrain [4], [13]. Most vertical parallax occurs when using a converged camera configuration, which induces keystone distortion. In addition, the range of acceptable vertical parallax induced by keystone distortion was discussed in [13], while [4] provided the amount of vertical parallax induced by a vertical shift.

A number of investigations have been conducted to measure the quality of stereoscopic images and videos. The International Telecommunications Union has recommendations for stereoscopic pictures [14]. Symptoms of visual fatigue are measured subjectively by assessing eyestrain, difficulty in focusing or blurred vision, stiff shoulders, and headaches [15]. Other methods for measuring visual fatigue, including accommodation, visual acuity, pupil diameter, and task performance were compared in [16].

Although subjective assessment is the most reliable method for gathering quality information from images and videos, it is expensive and time consuming. In this letter, we propose a visual fatigue prediction metric for stereoscopic images by measuring excessive horizontal and vertical disparities. The rest of this letter is organized as follows. First, we demonstrate backgrounds in Sections II and III. In Section IV, we propose five visual fatigue prediction metrics. Experimental results and conclusions are provided in Sections V and VI, respectively.

II. Backgrounds

Fig. 1 shows a stereoscopic geometry according to both shooting conditions and viewing conditions. We demonstrate stereoscopic imaging and display systems of a parallel camera without any distortions. For a converged camera configuration, the converging angles should also be considered and which are

Manuscript received December 11, 2009; revised April 2, 2010, May 26, 2010 and September 16, 2010; accepted September 26, 2010. Date of publication January 17, 2011; date of current version March 2, 2011. This work was supported in part by the IT R&D Program of MKE/KCC/KEIT [10035158, quality monitoring and quality assurance for multimedia and 3-D applications] and in part by the MKE, Korea, under the ITRC Support Program supervised by the NIPA (NIPA-2010-C1090-1001-0006). This paper was recommended by Associate Editor S. Yan.

The authors are with the Department of Electrical and Electronic Engineering, Yonsei University, Seoul 120-749, Korea (e-mail: khsohn@yonsei.ac.kr).

Digital Object Identifier 10.1109/TCSVT.2011.2106275

well defined in [13]. The geometry of the stereoscopic system shown in Fig. 1 contains camera coordinates and display coordinates, both of which are in 3-D space. Among the camera and display coordinates, sensor, image, and monitor coordinates are also considered. P_c and P_d represent the 3-D point in camera and display coordinates, respectively. f, B, and h represent the focal length, baseline, and sensor/image shift, respectively. The sensor/image shift is introduced in a parallel camera to generate both negative and positive parallaxes. In addition, $P_s(X_s, Y_s)$, $P_m(X_m, Y_m)$, and $P_i(X_i, Y_i)$ represent the X and Y positions of the sensor, monitor, and image coordinates, respectively. In addition, P_v represents viewer position.

Equation (1) allows for a change in coordinates from camera coordinates to sensor coordinates, or vice versa. In addition, (2) shows the relationship between the sensor and monitor coordinates, while (3) shows the relationship between the monitor and image coordinates as follows:

$$X_{sl} = f \times \left(\frac{B/2 + X_c}{Z_c}\right) - h,\ X_{sr} = -f \times \left(\frac{B/2 - X_c}{Z_c}\right) + h,\ Y_s = \frac{Y_c \times f}{Z_c} \tag{1}$$

$$X_m = M \times X_s,\ Y_m = M \times Y_s \tag{2}$$

where M is the screen magnification factor as follows:

$$X_m = (X_i - \frac{col}{2}) \times \frac{width_m}{col},\ Y_m = (Y_i - \frac{row}{2}) \times \frac{height_m}{row} \tag{3}$$

where row and col represent the resolution and $width_m$ and $height_m$ represent the size of the monitor.

Distances of r and l in camera coordinates indicate sensor disparity, which will be denoted as $Disp_s$, while the distances in display coordinates indicate monitor disparity, which will be denoted as $Disp_m$. Both of these values are scaled according to the ratio of monitor size to sensor size as shown in (4) and (5) as follows:

$$Disp_s = X_{sr} - X_{sl} \tag{4}$$

$$Disp_m = X_{mr} - X_{ml} = M \times Disp_s. \tag{5}$$

Perceived depth in the display coordinates can be calculated from the monitor coordinates by using two similar triangles and the equation as follows:

$$X_d = \frac{I}{I - Disp_m} \times \frac{X_{mr} + X_{ml}}{2},\ Y_d = \frac{I \times Y_m}{I - Disp_m},\ Zd = \frac{Disp_m \times V}{Disp_m - I} \tag{6}$$

where I, V, and $Disp_m$ represent the inter-ocular distance, the viewing distance, and the disparity of the monitor, respectively.

III. Disparity Estimation

Disparity estimation can be classified into sparse or dense matching. Dense correspondences that are established for every pixel of an image and many dense matching algorithms have been proposed [17]. However, each pixel cannot always be reliably matched in low-textured or occluded regions. In contrast, sparse disparity estimations are established between distinct spots in the images. Usually, they match with subpixel precision and, therefore, are reliable. However, sparse features may not represent the characteristics of the entire image.

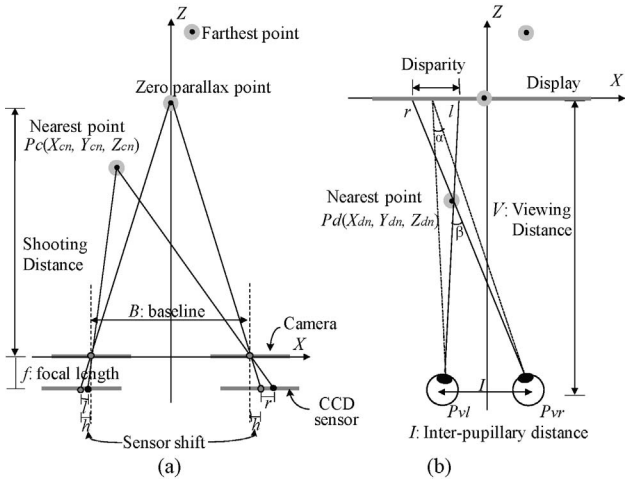

Fig. 1. Geometry of a stereoscopic system. (a) Camera. (b) Display coordinates.

Therefore, we performed several experiments on both sparse and dense methods. For sparse corresponding feature, we utilized the scale-invariant feature transform (SIFT), a sparse matching algorithm, to extract the feature disparity value [18], [19]. In addition, Kanade–Lucas–Tomasi feature tracker is tested which is matched to the features by comparing their similarity values [20]. Then, we utilized two dense disparity estimation algorithms which are dynamic programming and region-dividing technique with energy-based regularization [17], [21]. Finally, we choose features with the best results which are SIFT for sparse feature and region-dividing technique with energy-based regularization for dense disparity.

In general, disparities are the differences in image coordinates, as measured in pixels. It can be calculated using (7) and (8) for the x and y axes as follows:

$$Disp_{ix} = X_{ir} - X_{il} \tag{7}$$

$$Disp_{iy} = Y_{ir} - Y_{il}. \tag{8}$$

However, the actual perceived depth value cannot be calculated from pixel disparities because it varies with changes in viewing conditions. Angular disparities are widely used because they take into account the viewing conditions. It is the difference between the converging angles of the 3-D object and the screen. However, the results vary if the viewer changed position or if multiple viewers exist at the same time. Therefore, we utilized angular disparities which consider the locations of features and can be calculated as the difference between the angle between a 3-D feature and the viewer's eye and the angle between the feature in the monitor and the viewer's eye, the difference in the angles α and β in Fig. 1(b). Vectors $\vec{a}$, $\vec{b}$, $\vec{c}$, and $\vec{d}$ are shown in (9) and (10), where

P_v, P_{vl}, and P_{vr} represent the positions of the viewer, the left eye and the right eye, respectively. The angular disparities can then be calculated using (11). Then, we separate the values into horizontal and vertical disparity which are $Dispa_h$ and $Disp_{av}$ as follows:

$$\begin{aligned}\overrightarrow{a} &= P_{vl} - P_{dl} = (x_v - I/2 - x_{dl}, y_v - y_{dl}, z_v - z_{dl})^{\mathrm{T}} \\ \overrightarrow{b} &= P_{vr} - P_{dr} = (x_v + I/2 - x_{dr}, y_v - y_{dr}, z_v - z_{dr})^{\mathrm{T}} \end{aligned} \quad (9)$$

$$\overrightarrow{c} = P_{vl} - (P_{dl} + P_{dr})/2,\ \overrightarrow{d} = P_{vr} - (P_{dl} + P_{dr})/2 \quad (10)$$

$$Disp_a = \cos^{-1}\left(\frac{\overrightarrow{a}\cdot\overrightarrow{b}}{|\overrightarrow{a}|\cdot|\overrightarrow{b}|}\right) - \cos^{-1}\left(\frac{\overrightarrow{c}\cdot\overrightarrow{d}}{|\overrightarrow{c}|\cdot|\overrightarrow{d}|}\right). \quad (11)$$

After calculating the angular disparities from every feature in a stereoscopic image pair, we apply a filtering method to reduce the effect of matching errors by RANSAC algorithm using the constraint of the fundamental matrix.

IV. Visual Fatigue Prediction Using Sparse and Dense Corresponding Features

In the previous section, we examined how to extract reliable corresponding features and various kinds of disparities. Our goal is to predict visual fatigue induced from excessive horizontal and vertical disparities due to inadequate shooting parameters or camera misalignment. We basically utilize angular disparity to extract the disparity characteristics in the horizontal and vertical directions. In addition, we consider the change in the fusional limit according to the spatial frequency of images for horizontal disparities and the modeling of keystone distortion for vertical disparities. Then, five metrics are presented as combinations of these methods.

A. Extracting the Characteristics of Horizontal Disparities

Horizontal disparity is the most important factor because it directly affects perceived depth and visual fatigue with respect to several shooting parameters (baseline, focal length shooting distance, resolution) and several viewing parameters (viewing distance, resolution, display size).

A number of investigations have been conducted to determine the fusional limit of horizontal disparity. The 3-D Consortium [6] recommended that disparity be maintained at less than ± 60 arcmin. Nojiri *et al.* [11] insisted that the range of angular disparities should be limited to less than 60 arcmin. In addition, Kooi and Toet [5] suggested that disparity should not exceed 30 arcmin.

In this letter, we investigate the effects of horizontal and vertical disparities on visual fatigue and seek to determine which method best describes each factor, rather than to figure out an accurate fusional limit. We present three methods for extracting the characteristics of horizontal disparity.

1) *Method 1. Range of Pixel Disparities [18]:* Equation (12) measures the disparity ranges from a stereoscopic image. The horizontal disparities of the features are ordered to simplify the equation. In (12), $Disp(f)$ represents the maximum disparity and $Disp(f_n - f)$ represents the minimum disparity of the sparse horizontal disparities, and the difference between them is the range of disparity. Note that we set the upper and lower ranges when we sum the feature values, in order to decrease the effect of errors occurring from disparity estimation. After filtering is applied to the corresponding features using constraints of the fundamental matrix, it is possible to use the higher upper and lower ranges, which are closer to the accurate maximum and minimum disparity values as follows:

$$\mathrm{Range}_{\mathrm{h1}} = \sum_{f=fn\times f_1}^{fn\times f_2} (Disp_{ih}(f) - Disp_{ih}(fn - f)) \quad (12)$$

where $Disp_{ih}(f)$, f_n, f_1, and f_2 represent in order the horizontal disparity, the number of features, and the upper and lower ranges in percent, respectively.

2) *Method 2. Range and Maximum Angular Disparities Considering the Locations of the Features:* For the second method, we calculate the range and the maximum angular disparity of each feature considering the locations of the features. The major difference between methods 1 and 2 is the use of a maximum disparity value rather than only using a disparity range. The maximum disparity value is an important factor because it induces the conflict between accommodation and convergence in stereoscopic vision. In addition, angular disparity considers the locations of features, defined by (11). We integrated the angular disparities of the features which exceed the threshold value using (13) and (14) as follows:

$$\mathrm{Max}_{\mathrm{h2}} = \sum_{f=fn\times f_1}^{fn\times f_2} Disp_{ah}(f), \quad if\ |Disp_{ah}(f)| > th_{ah} \quad (13)$$

$$\mathrm{Range}_{\mathrm{h2}} = \sum_{f=fn\times f_1}^{fn\times f_2} (Disp_{ah}(f) - Disp_{ah}(fn - f)), \quad \text{if } |Disp_{ah}(f)| > th_{ah}. \quad (14)$$

3) *Method 3. Range and Maximum Angular Disparity Considering the Location and Spatial Frequency:* The third method considers changes in the fusional limit according to the spatial frequencies of the features based on the second method. We utilized the fact that visual information processed by the brain is sensitive to spatial frequency. The relationship between visual comfort and disparity with regard to local frequency is shown in [8]. Spatial frequency is measured in cycles per degree (cpd), the number of repetitions of a periodic pattern within a width of one degree. We obtained a spatial frequency component of the stereoscopic images by applying the Sobel operation because measuring the cpd is not possible in natural images. Then, we simplified the graph in [8] such that visual fatigue increases with the increase of disparity and also linearly increases according to spatial frequency. To accomplish this simplification, we multiplied a scale factor $S(f)$ by the angular disparity values so that the features which contained a large disparity and a high frequency had a greater

affect on the predicted visual fatigue. The third method is calculated using (15)–(17) as follows:

$$s(f) = 1 + \lambda \times \frac{Sobel(f)}{255} \tag{15}$$

$$\mathrm{Max}_{\mathrm{h3}} = \sum_{f=fn\times f_1}^{fn\times f_2} Disp_{ah}(f) \times S(f), \quad if \ |Disp_{ah}(f)| > th_{ah} \tag{16}$$

$$\mathrm{Range}_{\mathrm{h3}} = \sum_{f=fn\times f_1}^{fn\times f_2} (Disp_{ah}(f) \times S(f)) - \sum_{f=fn\times f_1}^{fn\times f_2} (Disp_{ah}(fn-f) \times S(fn-f)), \quad \text{if } |Disp_{ah}(f)| > th_{ah}. \tag{17}$$

B. Extracting the Characteristics of Vertical Disparities

Vertical disparity is a well-known visual fatigue-causing problem. A number of studies have been conducted to determine the effects of vertical disparity, and some of the research has provided an amount of acceptable vertical parallax by subjective evaluation. Woods *et al.* indicated that corresponding points in display coordinates should have less than 7 mm of vertical parallax in order to allow image fusion to be possible [13]. In addition, Kooi and Toet [5] provided a limit of vertical disparity induced by vertical shift and keystone distortion. The results recommend that viewing comfort will not be reduced for keystone distortions up to 0.57 degrees. In this letter, we present three methods for extracting the characteristics of vertical disparities.

1) *Method 1. Pixel Disparities Range [18]:* Equation (18) shows how to measure the range of vertical disparity in a stereoscopic image. It adopts the same structure as in (17) and represents the difference between the upper average and the lower average of the ordered vertical disparity of each feature as follows:

$$\mathrm{Range}_{\mathrm{v1}} = \sum_{f=fn\times f_1}^{fn\times f_2} (Disp_{iv}(f) - Disp_{iv}(fn-f)) \tag{18}$$

where $Disp_{iv}(f)$ represents the ordered vertical disparity.

2) *Method 2. Range and the Maximum Angular Disparity Considering Feature Location:* For the second method, we calculated the range and maximum angular disparity of each feature by considering the location of features using a similar method to that of horizontal disparity. We summed the angular disparities of the features which exceeded the threshold value in order to measure the visual fatigue induced from the vertical disparity factor, as in (19) and (20). Note that the maximum disparity in (19) was determined by comparing the absolute value of the maximum disparity and the minimum disparity. In the case of vertical disparity, features with a large absolute disparity-induced visual fatigue regardless of the sign

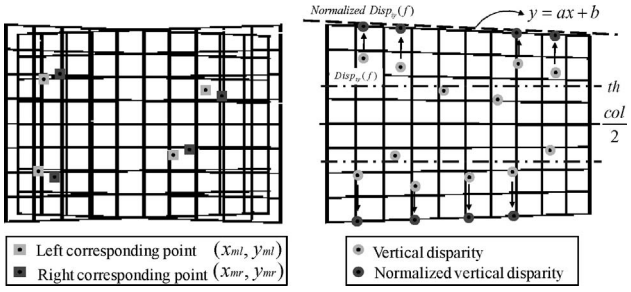

Fig. 2. Keystone distortion modeling.

as follows:

$$\mathrm{Max}_{\mathrm{v2}} = Max\left(\left|\sum_{f=fn\times f_1}^{fn\times f_2} Disp_{av}(f)\right|, \left|\sum_{f=fn\times f_1}^{fn\times f_2} Disp_{av}(fn-f)\right|\right) \quad if \ |Disp_{av}(f)| > th_{av} \tag{19}$$

$$\mathrm{Range}_{\mathrm{v2}} = \sum_{f=fn\times f_1}^{fn\times f_2} (Disp_{av}(f) - Disp_{av}(fn-f)) \quad \text{if } |Disp_{av}(f)| > th_{av}. \tag{20}$$

3) *Method 3. Keystone Distortion Modeling:* Most vertical parallax occurs in the converged camera configuration, which induces keystone distortion. Keystone distortion is the phenomenon that in one of the views, the image of the grid appears larger at one side than the other as shown in Fig. 2. We modeled keystone distortion with a line equation, as shown in Fig. 2. The scale factor of each feature is determined by (21) which normalizes the distance between feature and center line of the image. Then, we multiplied the scale factor by vertical disparity of corresponding features, whose value of y-axis is larger than threshold to reduce normalization errors as follows:

$$S_{keystone}(f) = \frac{col/2}{|col/2 - Y_i(f)|} \tag{21}$$

$$Normalized\_Disp_{iv}(f) = S_{keystone}(f) \times Disp_{iv}(f) \quad \text{if } Y_i(f) > th \tag{22}$$

where $X_i(f)$, $Y_i(f)$, and $Disp_{iv}(f)$ represent the location (x-axis, y-axis) and vertical disparity of the feature, respectively.

As we have a number of matching features, we can estimate a line equation ($y = ax + b$) according to the least squares method by using $X_i(f)$ as x and $Normalized\ Disp_{iv}(f)$ as y. The arc tangent values of slope a and y-intercept b are representative of the keystone distortion modeling from the third method. If vertical shift is detected in the stereoscopic images, one can simply translate one of the stereoscopic images and crop them into an image of the same resolution. In the case of keystone distortion, image rectification can be applied to stereoscopic images.

C. Predicting the Overall Visual Fatigue

In this section, we present a combined scheme using the horizontal and vertical disparities to predict the overall visual fatigue. Since horizontal and vertical disparities showed

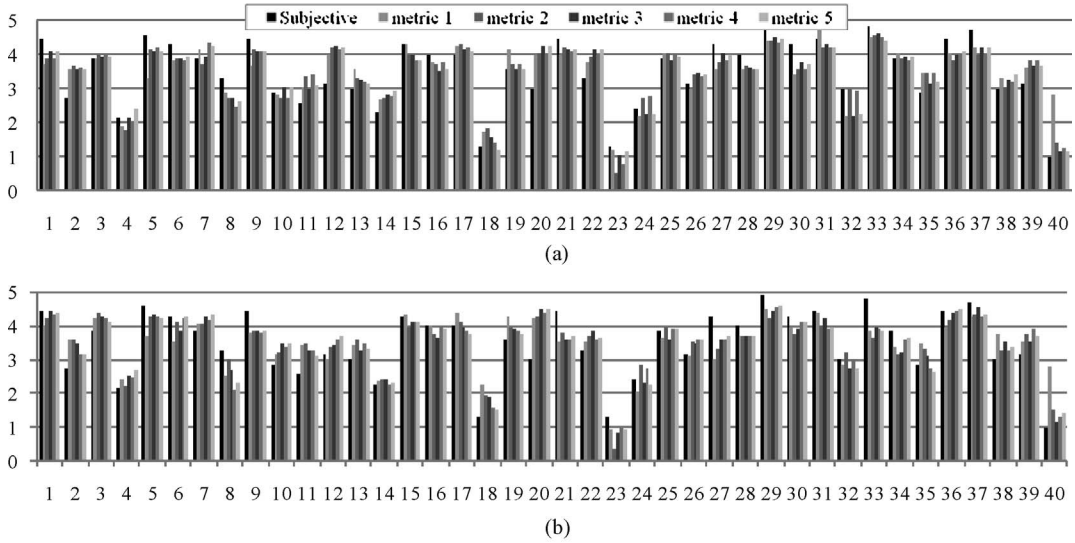

Fig. 3. Results for the visual fatigue prediction metrics. (a) Visual fatigue of image with sparse features. (b) Visual fatigue of image with dense features.

TABLE I
COMBINATIONS OF THE PROPOSED METRICS

	Horizontal Characteristics	Vertical Characteristics
Metric 1	H. Method 1	V. Method 1
Metric 2	H. Method 2	V. Method 2
Metric 3	H. Method 2	V. Method 3
Metric 4	H. Method 3	V. Method 2
Metric 5	H. Method 3	V. Method 3

TABLE II
COMPARISON OF THE CORRELATIONS OF THE PROPOSED METRICS

	Metric 1	Metric 2	Metric 3	Metric 4	Metric 5
Sparse feature (%)	78.85	85.15	87.65	85.85	86.82
Dense feature (%)	74.64	81.13	84.72	85.14	85.92

independence in [18], we used additive first-order linear regression. Linear regression coefficients were calculated using a least squares method, which maximizes Pearson's correlation between the predicted visual fatigue and the subjective visual fatigue. We utilized k-fold cross-validation when measuring the correlation [22]. Then, we evaluated the performances of the five metrics of visual fatigue prediction, which are combinations of the proposed methods as shown in Table I.

V. EXPERIMENTAL RESULTS

Twenty-four inch polarized stereoscopic display was used for the subjective assessment. Twenty nonexpert assessors, aged 22 to 34, participated in the subjective assessment. They watched randomly ordered stereoscopic images for 8 s at a distance of 1 m from the monitor [14]. In our experiment, we used a five-level scale including ratings of no fatigue, slight fatigue, moderate fatigue, fatigue, and severe fatigue [12]. In order to evaluate the proposed algorithm, 40 stereoscopic images were used, consisting of 18 outdoor scenes, 14 indoor scenes, and eight computer graphic scenes [23].

Fig. 3 shows the results of the predicted visual fatigue for whole stereoscopic images using Metrics 1–5. We analyzed the characteristics of stereoscopic images which showed a difference between the subjective and predicted results. In most cases, the horizontal and vertical disparities were sufficient to predict the visual fatigues of the images. However, feature errors occurred from repeated patterns and lack of texture for both sparse and dense feature. Moreover, frame effect, depth distortion, and image imperfections such as synchronization should be carefully considered.

We measured the correlation of the predicted results with the subjective results in order to validate our metrics, and the results are shown in Table II. Sparse feature showed a relatively high correlation than that of dense feature. It is due to the nature of dense features that errors from low-textured and occluded area usually appeared in relatively large region. It leads to poor fundamental matrix and lower correlation. In addition, Metric 3 and Metric 5, which utilized angular disparity and keystone distortion modeling, showed the best performances for both features, while Metric 1, which utilized pixel disparity, showed the worst performance among the five metrics.

VI. CONCLUSION

In this letter, we proposed a visual fatigue metric which could predict the levels of visual fatigue from stereoscopic images. The prediction of the visual fatigues of stereoscopic images can be used in various applications such as substituting subjective evaluations, filming aid systems, and in warning systems for general viewers. We are currently researching an accurate dense disparity estimation algorithm which is robust to stereoscopic impairments such as vertical disparities or color differences because sparse features may not represent the characteristics of the entire image. If such an algorithm is feasible, visual fatigue level and picture quality could be

assessed simultaneously. In future works, we will extend our research to address factors which affect visual fatigue such as temporal depth variation, motion, contrast, and focus.

REFERENCES

[1] G. Jones, D. Lee, N. Holliman, and D. Ezra, "Controlling perceived depth in stereoscopic images," *Proc. SPIE*, vol. 4297A, pp. 42–53, Jun. 2001.

[2] S. Yano, S. Ide, T. Mitsuhashi, and H. Thwaites, "A study of visual fatigue and visual comfort for 3-D HDTV/HDTV images," *Displays*, vol. 23, no. 4, pp. 191–201, Sep. 2002.

[3] N. Hiruma and T. Fukuda, "Accommodation response to binocular stereoscopic TV images and their viewing conditions," *SMPTE J.*, vol. 102, no. 12, pp. 1137–1144, 1993.

[4] W. Ijsselsteijn, H. Ridder, and J. Vliegen, "Subjective evaluation of stereoscopic images: Effects of camera parameters and display duration," *IEEE Trans. Circuits Syst. Video Technol.*, vol. 10, no. 2, pp. 225–233, Mar. 2000.

[5] F. Kooi and A. Toet, "Visual comfort of binocular and 3-D displays," *Displays*, vol. 25, pp. 99–108, Aug. 2004.

[6] C. Shigeru, "3-D consortium safety guidelines for popularization of human-friendly 3-D," *Eizo Joho Media Gakkai Gijutsu Hokoku*, vol. 30, no. 34, pp. 21–24, 2006.

[7] E. Jin, M. Miller, S. Endrikhovski, and C. Cerosaletti, "Creating a comfortable stereoscopic viewing experience: Effects of viewing distance and field of view on fusional range," *Proc. SPIE*, vol. 5664A, pp. 10–21, 2005.

[8] M. Wöpking, "Viewing comfort with stereoscopic pictures: An experimental study on the subjective effects of disparity magnitude and depth of focus," *J. SID*, vol. 3, no. 3, pp. 101–103, 1995.

[9] H. Yamanoue, S. Ide, M. Okui, F. Okano, M. Bitou, and N. Terashima, "Parallax distribution for ease of viewing in stereoscopic HDTV," NHK Laboratories, Inc., Tokyo, Japan, Tech. Rep. 477, 2002.

[10] W. Ijsselsteijn, H. Ridder, R. Hamberg, D. Bouwhuis, and J. Freeman, "Perceived depth and the feeling of presence in 3-DTV," *Displays*, vol. 18, no. 4, pp. 207–214, 1998.

[11] Y. Nojiri, H. Yamanoue, A. Hanazato, M. Emoto, and F. Okano, "Visual comfort/discomfort and visual fatigue caused by stereoscopic HDTV viewing," *Proc. SPIE*, vol. 5291, pp. 303–313, Jan. 2004.

[12] M. Emoto, Y. Nojiri, and F. Okano, "Changes in fusional vergence limit and its hysteresis after viewing stereoscopic TV," *Displays*, vol. 25, nos. 2–3, pp. 67–76, Aug. 2004.

[13] A. Woods, T. Docherty, and R. Koch, "Image distortions in stereoscopic video systems," *Proc. SPIE*, vol. 1915, pp. 36–48, Feb. 1993.

[14] ITU-R, "Subjective assessment of stereoscopic television pictures," document ITU Rec. BT.1438, 2000.

[15] A. Suzumura, "Visual fatigue," *Ganka*, vol. 23, no. 8, pp. 799–804, 1981.

[16] C. Chi and F. Lin, "A comparison of seven visual fatigue assessment techniques in three data-acquisition VDT tasks," *Human Factors*, vol. 40, no. 4, pp. 577–590, 1998.

[17] D. Sharstein and R. Szeliski, "A taxonomy and evaluation of dense two-frame stereo correspondence algorithms," in *Proc. IEEE Workshop Stereo Multi-Baseline Vision*, Dec. 2001, pp. 131–140.

[18] D. Kim, D. Min, J. Oh, S. Jeon, and K. Sohn, "Depth map quality metric for 3-D video," *Proc. SPIE*, vol. 7237, pp. 191–199, 2009.

[19] D. G. Lowe, "Distinctive image features from scale-invariant keypoints," *Int. J. Comput. Vision*, vol. 60, no. 2, pp. 91–110, 2004.

[20] C. Tomasi and T. Kanade, "Detection and tracking of point features," Carnegie Mellon University, Pittsburgh, PA, Tech. Rep. CMU-CS-91-132, 1991.

[21] H. Kim, Y. Choe, and K. Sohn, "Disparity estimation using region-dividing technique with energy-based regularization," *Optic. Eng.*, vol. 43, no. 8, pp. 1882–1890, 2004.

[22] M. Green and M. Ohlsson, "Comparison of standard resampling methods for performance estimation of artificial neural network ensembles," in *Proc. Computat. Intell. Med. Healthcare*, 2007.

[23] Yonsei University. (2010). [Online]. Available: http://diml.yonsei.ac.kr/dhkim